J|A|C|S COMMUNICATIONS

Published on Web 04/02/2010

A Small-Molecule-Based Ternary Data-Storage Device

Hua Li, Qingfeng Xu, Najun Li, Ru Sun, Jianfeng Ge, Jianmei Lu,* Hongwei Gu,* and Feng Yan

Key Laboratory of Organic Synthesis of Jiangsu Province, College of Chemistry, Chemical Engineering and Materials Science, Soochow University, Suzhou 215123, China

Received December 4, 2009; E-mail: lujm@suda.edu.cn; hongwei@suda.edu.cn

Currently, most data-storage systems based on semiconductors[1] or optical[2] or magnetic[3] materials are binary and have two output signals: 0 and 1. To achieve high-density data storage (HDDS), physical scaling limitations (simply reducing the bit cell size[4]) have been adopted by most scientists. Nowadays, although the theoretical data density has increased to the terabit scale while the domain size has been scaled down to the nanometer scale,[5] many new problems such as difficulties in nanofabrication and data writing and reading[6] have hindered the development of HDDS devices. Another effective alternative for increasing data storage is to increase the number of memory states in each cell (i.e., to have memory states 0, 1, 2, ...). Such devices have been less-explored,[7] partly because of the lack of appropriate materials. The Agarwal group first reported the ternary storage behavior of $Ge_2Sb_2Te_5$/GeTe core/shell nanowires, which contain two phase-change materials with different electronic and thermal properties and thus have three distinct electronic states. In the last several years, the Scott,[8] Huang,[9] Kang,[10] and Ree[11] groups have reported sandwich-structured memory devices fabricated using polymeric materials containing electron-donor and -acceptor moieties that exhibit good electric bistable behavior with an ON/OFF current ratio of 10^4-10^6. Herein, we report the fabrication of a prototype ternary memory device with a novel small organic molecule as the active material. The molecule exhibits promising ternary behavior under an electric field, increasing the data-storage capacity of the device from 2^n to 3^n.

Scheme 1. Molecular Structures of *Azo1−4*

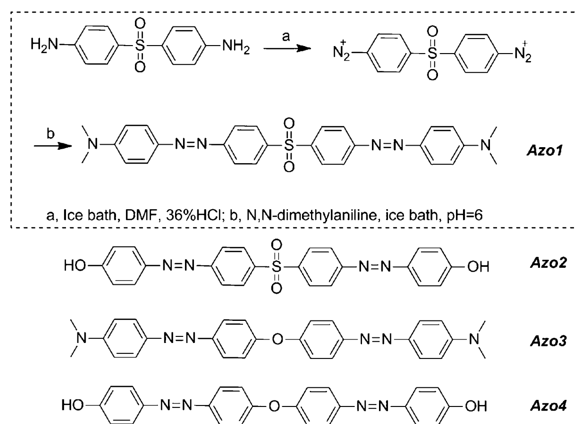

Compound *Azo1* was synthesized by the reaction of *N*,*N*-dimethylaniline with a diazonium salt (Scheme 1). The *Azo1* molecule is symmetric about the sulfone group and has two 4′-(*N*,*N*-dimethylaminoazobenzene) components. Compounds *Azo2−4* were synthesized as controls and have structures similar to that of *Azo1*.[12]

Figure 1A illustrates the structure of our prototype memory device, which is a sandwich structure comprising a pair of electrodes and a layer of *Azo* film. *Azo* molecules were deposited on an indium tin oxide (ITO) substrate (∼20 nm) via vacuum deposition at 3 × 10^{-4} Pa. The film thickness was about 75 nm, as measured by scanning electron microscopy through a cross section of the film (Figure 1C). Al top electrodes (0.2 mm diameter and 80 nm thickness) were thermally deposited on the film with a mask and are easily identified in Figure 1B.

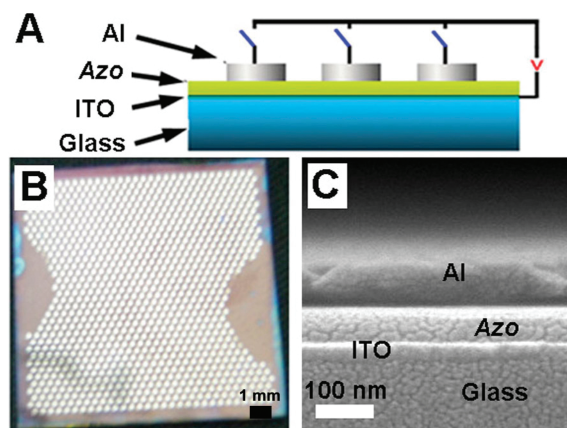

Figure 1. (A) Illustration of the sandwich device. (B) Optical image of the prototype device. (C) SEM image of a cross section of the device.

The current−voltage (*I−V*) characteristics of the device were determined using an HP 4145B semiconductor parameter analyzer. Figure 2A shows the *I−V* performance of the device fabricated with *Azo1*. In the first sweep from 0 to −3.0 V, two abrupt increases in current were observed at switching threshold voltages (STVs) of −1.37 and −2.09 V, indicating the transitions from a low-conductivity ("0") state to an intermediate-conductivity ("1") state and then to a high-conductivity state ("2"). The cell remained in this high-conductivity ("2") state during the subsequent scan from 0 to −3 V (sweep 2). Sweep 3 was the measurement of another cell of the device over a voltage range of 0 to −1.7 V and showed one STV at −1.45 V. The intermediate-conductivity state ("1") was maintained during the subsequent scan from 0 to −1.7 V (sweep 4). These two actions represent the process of "writing" the memory device. It is worth mentioning that our device is highly stable after proper data writing and that a constant voltage (−1.0 V, for example) can be employed to read the "0" (low-conductivity), "1" (intermediate-conductivity), and "2" (high-conductivity) signals of the memory device (Figure 2B). The stability performance of our device based on *Azo1* was evaluated, and Figure 2B shows the device performance under continuous stress. There is no significant degradation in any of the three states. The three states of the ternary memory cell are distinct; the current ratio of the "0", "1", and "2" states is $1:10^2:10^6$. This device exhibits typical write-once read-many-times (WORM) behavior. The "writing" voltage is between 0 and −3 V, and the "reading" voltage is between 0.25 and −1.3 V. The *I−V* performances of *Azo2−4* were measured under the same conditions. *Azo2* showed no distinct current change as the voltage

10.1021/ja910243f © 2010 American Chemical Society

was reduced from 0 to −4 V. *Azo3* and *Azo4* had binary data storage behaviors with operation voltages of −1.7 and −3.6 V, respectively.[12]

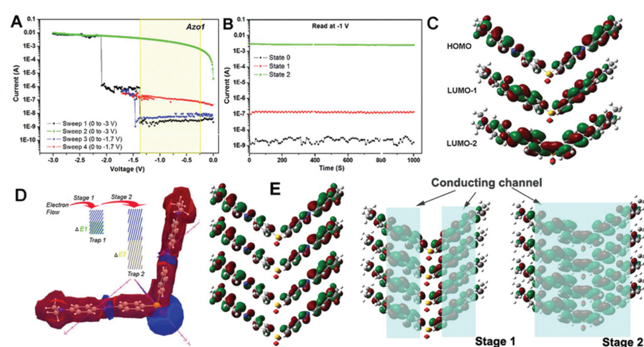

Figure 2. (A) *I*−*V* characteristics of the memory device fabricated with *Azo1*. (B) Stability of the device in three states under a constant "read" voltage of −1 V. (C) DFT molecular simulation results (B3LYP/6-311G* level): LUMO-1, LUMO-2, HOMO. (D) Molecular simulation results for ESP surfaces of *Azo1* and the proposed electron-flow mechanism at molecular level. (E) Molecular stacking model and illustrations of the conducting channels of the stacking molecules.

To determine the *I*−*V* performance, the structures of *Azo1*−*4* were analyzed using density functional theory (DFT) molecular simulations. Highest unoccupied molecular orbital (HOMO) and lowest unoccupied molecular orbital (LUMO) calculations (Figure 2C) demonstrated that the electron density at the azo group increases with electron injection (LUMO-1) and that further injection of electrons increases the electron density at the sulfone group (LUMO-2) to form an free path for electrons along the whole molecule. Figure 2D shows the electrostatic potential (ESP) of the *Azo1* molecule. The molecule surface has a continuous positive ESP (in red) along the conjugated backbone, which indicates that charge carriers can migrate through this open channel. However, there are negative ESP regions (blue lobes) caused by electron-acceptor groups. These negative regions can serve as "traps" that impede the mobility of the charge carriers. The electron-flow mechanism at molecular level is also illustrated in Figure 2D. In the first stage, electrons fill the first trap. When the applied voltage is increased to −1.4 V, $\Delta E1$ increases, making the first trap sufficiently shallow for the molecules to become partially conductive. As the applied voltage is increased to −2.1 V, $\Delta E2$ reaches a maximum, and the whole molecule becomes conductive.

X-ray diffraction (XRD) analysis was carried out to clarify the conduction mechanism at the device level. The XRD results (Figure S3 in the Supporting Information) show that the *Azo1* film has two sharp diffraction peaks at 29.9 and 34.9°. These peaks show the planar distance of the aromatic rings and demonstrate that the molecules are well-stacked. We further checked the XRD of the thin film after adding an external voltage of 3 V and found that the peaks shifted to 30.6 and 35.5°, demonstrating that the planar distance between the aromatic rings is reduced and thus that the molecular stacking is denser. The molecular packing model and thin-film conduction mechanism are shown in Figure 2E. Shortening of the distance of the aromatic rings generates two free paths for electrons at LUMO-1 via intermolecular interactions, resulting in a partially conductive thin film. At LUMO-2, the whole *Azo1* molecule becomes conductive, and a broad electron path forms via intermolecular interactions, resulting in a fully conductive thin film. The film thickness and size of the unit cell have little effect on the *I*−*V* performance of the device, and the same phenomenon was observed for different dimensions (Figure S5).

Figure 3 shows the ternary data storage performance of our prototype device fabricated with *Azo1*. We selected 18 cells of the device, and each cell was written as 0 or 1 or 2. Cells were combined into nine pairs and could be read as 00, 01, 02, 10, 11, 12, 20, 21, and 22 (i.e., *ab* in ternary). These signals can be easily identified as 0, 1, 2, 3, 4, 5, 6, 7, and 8 (i.e., *N* in decimal) following the simple equation $N = a \times 3^1 + b \times 3^0$. Compared with a traditional binary system, the capacity of our device increased from 2^n to 3^n.

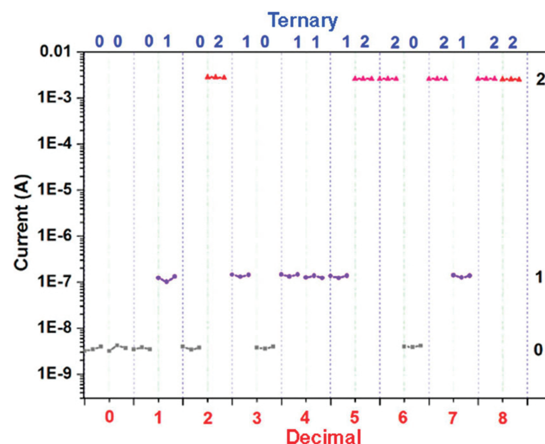

Figure 3. Ternary data storage performance of our prototype device. All of the measurements were conducted under ambient conditions.

In summary, we fabricated a small-molecule (*Azo1*)-based device that has unexpected ternary *I*−*V* performance under a constant reading voltage. This prototype device consumes less power and is easier to scale than traditional devices. We believe that our result is promising for the development of an ideal ternary memory system and will open the door to the development of next-generation HDDS devices.

Acknowledgment. This work was partially supported by the Chinese Natural Science Foundation (20876101, 20902065), the Natural Science Foundation of Jiangsu Province (BK2008158), and the Supporting Program of Jiangsu Province (Industry) (BE2008061).

Supporting Information Available: Experimental details of molecule synthesis and memory device fabrication, *I*−*V* performance data, results of ESP calculations for *Azo2*−*4*, and XRD analysis of the *Azo1* film. This material is available free of charge via the Internet at http://pubs.acs.org.

References

(1) (a) Moller, S.; Perlov, C.; Jackson, W.; Taussig, C.; Forrest, S. R. *Nature* **2003**, *426*, 166. (b) Rozenberg, M. J.; Inoue, I. H.; Sanchez, M. J. *Phys. Rev. Lett.* **2004**, *92*, 178302. (c) Ouyang, J.; Chu, C. W.; Szmanda, C. R.; Ma, L. P.; Yang, Y. *Nat. Mater.* **2004**, *3*, 918.
(2) Hagen, R.; Bieringer, T. *Adv. Mater.* **2001**, *13*, 1805. (b) Kawata, S.; Kawata, Y. *Chem. Rev.* **2000**, *100*, 1777. (c) Emmelius, M.; Pawlowski, G.; Vollmann, H. *Angew. Chem., Int. Ed. Engl.* **1989**, *28*, 1445.
(3) Wang, J. P. *Nat. Mater.* **2005**, *4*, 191. (a) Osaka, T.; Takai, M.; Hayashi, K.; Ohashi, K.; Saito, M.; Yamada, K. *Nature* **1998**, *392*, 796.
(4) (a) Guo, L. J.; Leobandung, E.; Chou, S. Y. *Science* **1997**, *275*, 649. (b) Lankhorst, M. H. R.; Ketelaars, B. S. M. M.; Wolters, R. A. M. *Nat. Mater.* **2005**, *4*, 347. (c) Alexe, M.; Harnagea, C.; Erfurth, W.; Hesse, D.; Gosele, U. *Appl. Phys. A: Mater. Sci. Process.* **2000**, *70*, 247. (d) Alexe, M.; Harnagea, C.; Visinoiu, A.; Hesse, D.; Gosele, U. *Scr. Mater.* **2001**, *44*, 1175. (e) Jiang, G. Y.; Michinobu, T.; Yuan, W. F.; Feng, M.; Wen, Y. Q.; Du, S. X.; Gao, H. J.; Jiang, L.; Song, Y. L. *Adv. Mater.* **2005**, *17*, 2170.
(5) Green, J. E.; Choi, J. W.; Boukai, A.; Bunimovich, Y.; Halperin, E. J.; Delonno, E.; Luo, Y.; Sheriff, B. A.; Xu, K.; Shin, Y. S.; Tseng, H. R.; Stoddart, J. F.; Heath, J. R. *Nature* **2007**, *445*, 414.
(6) Waser, R. *Nanoelectronics and Information Technology: Advanced Electronic Materials and Novel Devices*; Wiley-VCH: Weinheim, Germany, 2005.
(7) Jung, Y. W.; Lee, S. H.; Jennings, A. T.; Agarwal, R. *Nano Lett.* 20088, 2056.
(8) Scott, J. C. *Science* **2004**, *304*, 62.
(9) Xie, L. H.; Ling, Q. D.; Hou, X. Y.; Huang, W. *J. Am. Chem. Soc.* **2008**, *130*, 2120.
(10) Ling, Q. D.; Chang, F. C.; Song, Y.; Zhu, C. X.; Liaw, D. J.; Chan, D. S. H.; Kang, E. T.; Neoh, K. G. *J. Am. Chem. Soc.* **2006**, *128*, 8732.
(11) Choi, S. C.; Hong, S. H.; Cho, S. H.; Park, S.; Park, S. M.; Kim, O.; Ree, M. *Adv. Mater.* **2008**, *20*, 1766.
(12) See the Supporting Information.

JA910243F